catalysts

MDPI

Article

Efficient Photocatalytic Hydrogen Peroxide Production over TiO_2 Passivated by SnO_2

Guifu Zuo [1], Bingdong Li [1], Zhaoliang Guo [1], Liang Wang [2], Fan Yang [3], Weishu Hou [3], Songtao Zhang [4], Peixiao Zong [1], Shanshan Liu [1], Xianguang Meng [1,5,*], Yi Du [2], Tao Wang [6,*] and Vellaisamy A. L. Roy [5,7,*]

1 Hebei Provincial Key Laboratory of Inorganic Nonmetallic Materials, College of Materials Science and Engineering, North China University of Science and Technology, Tangshan 063210, China
2 Institute for Superconducting and Electronic Materials, Australian Institute for Innovative Materials, University of Wollongong, Wollongong, New South Wales 2500, Australia
3 TU-NIMS International Collaboration Laboratory, School of Materials Science and Engineering, Tianjin University, 92 Weijin Road, Tianjin 300072, China
4 Testing Center, Yangzhou University, Yangzhou 225009, China
5 Department of Materials Science and Engineering, City University of Hong Kong, Tat Chee Avenue, Kowloon, Hong Kong, China
6 College of Materials Science and Technology, Jiangsu Key Laboratory of Materials and Technology for Energy Conversion, Nanjing University of Aeronautics and Astronautics, Nanjing 210016, China
7 State Key Laboratory for THz and Millimeter Waves, City University of Hong Kong, Tat Chee Avenue, Kowloon, Hong Kong, China
* Correspondence: mengxg_materchem@163.com (X.M.); wangtao0729@nuaa.edu.cn (T.W.); val.roy@cityu.edu.hk (V.A.L.R.)

Received: 24 June 2019; Accepted: 15 July 2019; Published: 21 July 2019

Abstract: Photocatalysis provides an attractive strategy for synthesizing H_2O_2 at ambient condition. However, the photocatalytic synthesis of H_2O_2 is still limited due to the inefficiency of photocatalysts and decomposition of H_2O_2 during formation. Here, we report SnO_2-TiO_2 heterojunction photocatalysts for synthesizing H_2O_2 directly in aqueous solution. The SnO_2 passivation suppresses the complexation and decomposition of H_2O_2 on TiO_2. In addition, loading of Au cocatalyst on SnO_2-TiO_2 heterojunction further improves the production of H_2O_2. The in situ electron spin resonance study revealed that the formation of H_2O_2 is a stepwise single electron oxygen reduction reaction (ORR) for Au and SnO_2 modified TiO_2 photocatalysts. We demonstrate that it is feasible to enhance H_2O_2 formation and suppress H_2O_2 decomposition by surface passivation of the H_2O_2-decomposition-sensitive photocatalysts.

Keywords: H_2O_2; single electron ORR; SnO_2-TiO_2; passivation

1. Introduction

Hydrogen peroxide (H_2O_2) is a clean oxidant [1] that has wide applications in environmental purification and organic synthesis [2]. At present, H_2O_2 is industrially produced by the multi-step anthraquinone method, which consumes a lot of energy and organic solvent [3]. As an alternative to the anthraquinone method, direct photocatalytic synthesis of H_2O_2 has attracted widespread attention due to its mild reaction conditions, such as normal temperature and pressure under light irradiation. Many representative UV-light and visible-light active semiconductors (e.g., ZnO [4,5], C_3N_4 [6–9], $BiVO_4$ [10], etc.) have been verified as active materials for H_2O_2 production, particularly when proper cocatalysts are loaded on these semiconductors. An important feature of photocatalytic H_2O_2 formation is that it is accompanied by a decomposition process. TiO_2 is a widely used photocatalyst for synthesizing H_2O_2

directly from O_2 reduction in liquid phase under the irradiation of ultraviolet (UV) light [3,11–17], without using hydrogen. However, photocatalytic H_2O_2 synthesis with TiO_2 has a low formation reaction rate due to the catalytic decomposition [17,18]. Some studies have revealed the decomposition mechanism of H_2O_2 in aqueous TiO_2 suspension under UV irradiation [18–20]. Zhao et al. [18] reported that adsorption of H_2O_2 on TiO_2 will readily form surface peroxide complexes, which can be easily photodegraded with a zero-order kinetic process over TiO_2 even with the irradiation of visible light, thus leading to the decrease of H_2O_2 production. Therefore, in order to produce concentrated H_2O_2, on one hand, the formation rate of H_2O_2 should be increased, and on the other hand, the decomposition of H_2O_2 should be controlled.

Au is an active cocatalyst and has shown great potential in improving the performance of photocatalytic H_2O_2 production [15,16]. Tada et al. [15] reported enhancement of the photocatalytic activity of TiO_2 in producing H_2O_2 by Au cocatalyst loading. They also found that the formation of H_2O_2 was generally accompanied by decomposition. The concentration of H_2O_2 produced from the photocatalytic reduction of O_2 can also be increased by restricting its thermocatalytic decomposition through controlling the temperature and pH of the reaction solution [16]. Indeed, these studies improved H_2O_2 formation activity by suppressing the decomposition process by controlling the reaction condition. However, there is still no effective means of enhancing the intrinsic activity of photocatalysts for H_2O_2 production. It is well known that both the structures and band gaps of TiO_2 and SnO_2 are similar. They all consist of MO_6 octahedrons as the structural unit. The conduction band (CB) of SnO_2 (0 V vs. SHE) is more positive than that of the TiO_2 (−0.3 V vs. SHE) and it is possible to improve charge separation in a photocatalytic reaction when heterojunctions are formed by both oxides [21–23]. In this study, we prepared SnO_2-modified anatase TiO_2 (SnO_2-TiO_2) heterojunction using the molten salt method [24]. SnO_2 passivation suppressed H_2O_2 complexation and decomposition on the surface of TiO_2. Loading of Au nanococatalysts further remarkably enhanced the H_2O_2 formation rate.

2. Results and Discussion

2.1. Characterization of the Photocatalysts

Figure 1a shows the XRD patterns of 0.1% Au loaded SnO_2-TiO_2 obtained at different sintering temperatures. When the sintering temperature is 300 °C, almost no SnO_2 can be detected. It has been well documented that the melting point of LiCl-KCl eutectic of composition 61:39 is 352 °C [24]. Hence, the Sn precursor is impossible to dissolve by molten salt and SnO_2 cannot be formed on the TiO_2 at this temperature. The presence of SnO_2 can be identified when the sintering temperature reaches 400 °C. At a sintering temperature of 500 °C, the peak of SnO_2 becomes more obvious, implying higher modification of SnO_2. At the sintering temperature of 600 °C, anatase was partially transformed into a less active rutile phase [25]. The diffraction peaks of SnO_2 can be clearly identified with the increase in the Sn/Ti ratio (Figure 1b). The presence of SnO_2 and Au are certified by the EDX (Figure S1). STEM mapping images (Figure 1c–f) display that SnO_2 and Au are finely dispersed on the surface of TiO_2. Formation of such a SnO_2-TiO_2 heterojunction structure will improve the charge separation and photocatalytic activity [21–23].

As shown in Figure 1g, there are two prominent absorption bands in the UV-Vis spectra of Au/SnO_2-TiO_2. Besides the characteristic absorption bands of TiO_2 at 370 nm, the broad absorption bands in the visible region between 500 nm and 650 nm is due to the excitation of gold surface plasmon. In addition, the nanometal cocatalyst exhibit lattice fringes of 0.235 nm, which matches the interplanar spacing of Au (1 1 1) plane (Figure S2) [26]. The actual content of Au in 0.1% Au/SnO_2-TiO_2 was 0.106% by inductively coupled plasma mass spectrometry (ICP-MS).

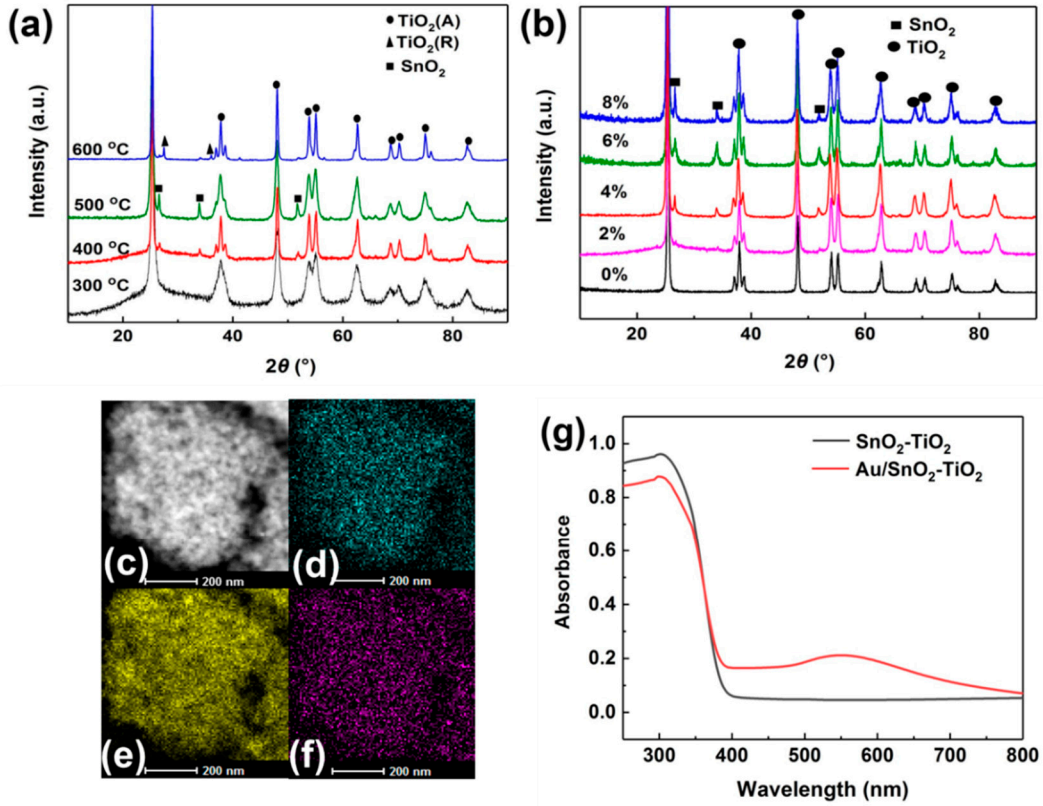

Figure 1. (**a**) XRD patterns of 0.1% Au loaded SnO_2-TiO_2 (4% SnO_2 modified anatase TiO_2) obtained at different sintering temperatures. (**b**) XRD patterns of 0.1% Au loaded SnO_2-TiO_2 with different Sn/Ti ratios. (**c**) HAADF-STEM images of 0.1% Au loaded SnO_2-TiO_2 (Sn/Ti is 4%). (**d**–**f**) Mapping images of (**d**) Sn, (**e**) Ti and (**f**) Au elements. (**g**) UV-vis spectra of SnO_2-TiO_2 with and without 0.1% Au.

2.2. Catalytic Activity of the Photocatalysts

The photocatalytic activity of H_2O_2 synthesis on Au/SnO_2-TiO_2 hybrids was tested under UV light and the concentration of H_2O_2 was quantified by spectrophotometry with copper ions and 2,9-dimethyl-1,10-phenanthroline (DMP) [27]. The standard curve indicates that the absorbance and concentration of H_2O_2 exhibits a good linear relationship with R square of 0.9996 (Figure S3). Figure 2a shows time courses for the H_2O_2 generation of photocatalysts obtained at different sintering temperatures. Noticeably, 0.1% Au loaded SnO_2-TiO_2 obtained at 500 °C exhibits the highest photocatalytic activity compared to that obtained at the other sintering temperatures. In combination with XRD data, when the sintering temperature is 300 °C, the content of SnO_2 in the samples is minimal, and the activity is not obviously improved. The photocatalytic activity of the samples obtained at 600 °C is the lowest, possibly because of the formation of a less active rutile phase.

Compared with pristine Au/TiO_2, Au/SnO_2-TiO_2 hybrids exhibited enhanced photocatalytic activity (Figure 2b). The highest photocatalytic activity was obtained over the sample with a Sn/Ti ratio of 4%, which also showed stable H_2O_2 production rate. The improved activity is mainly due to the suppression of H_2O_2 decomposition by SnO_2 passivation as discussed below. The excessive SnO_2 modification will possibly shield the photo absorption of TiO_2, and thus reduce the photocatalytic activity. It should be noted that we also did a control experiment, which is shown in Figure S4. It was found that there is a synergistic effect between Au and SnO_2 in H_2O_2 synthesis over TiO_2.

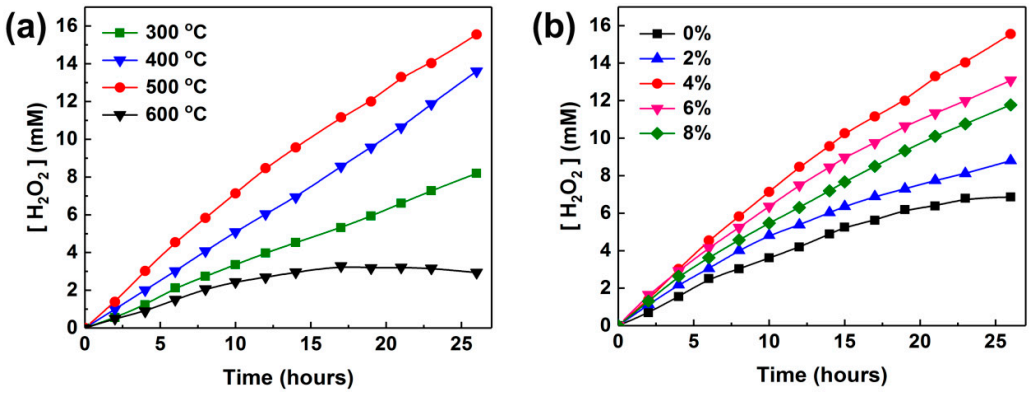

Figure 2. (**a**) Plots of [H_2O_2] under UV-irradiation in the presence of 0.1% Au loaded SnO_2-TiO_2 (4% SnO_2 modified anatase TiO_2) obtained at different sintering temperatures. (**b**) Plots of [H_2O_2] under UV-irradiation in the presence of 0.1% Au loaded SnO_2-TiO_2 with different Sn/Ti ratios.

2.3. ESR Analysis

In general, H_2O_2 from $2e^-$ ORR by CB electrons can be produced through stepwise coupled electron and proton transfers (Equations (1)–(3)) [28,29]. In order to further study the formation mechanism of H_2O_2, in situ ESR measurements were carried out using DMPO as the trapper of radical species. The radical signals of DMPO-•OOH consisting of six characteristic peaks were detected for all of Au and/or SnO_2 modified TiO_2, while there is no obvious signals for pure TiO_2 (Figure 3a,b), showing that H_2O_2 formation over Au loaded and/or SnO_2 modified TiO_2 photocatalysts is indeed a stepwise single electron reduction process, and both Au and SnO_2 could promote the formation of HO_2• via Equation (2).

$$TiO_2 \rightarrow e^- + h^+ \quad (1)$$

$$e^- + O_2 + H^+ \rightarrow HO_2\bullet \quad (2)$$

$$HO_2\bullet + H^+ + e^- \rightarrow H_2O_2 \quad (3)$$

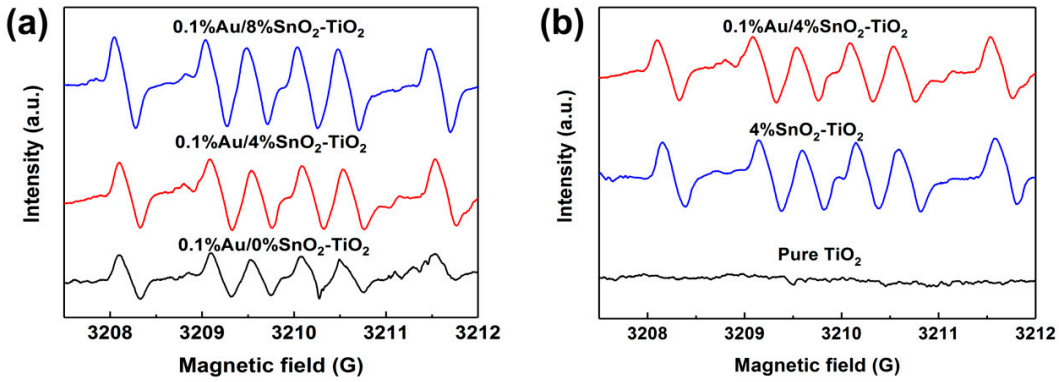

Figure 3. (**a**) In situ ESR spectra of the 0.1% Au/SnO_2-TiO_2 samples with different Sn/Ti ratios under UV light irradiation. (**b**) In situ ESR spectra of the samples (4% SnO_2 modified anatase TiO_2) with and without Au cocatalyst under UV light irradiation.

2.4. The Photodecomposition of H_2O_2

Figure 4 shows the decomposition of H_2O_2 under different conditions. Pure H_2O_2 remains stable under dark conditions in the presence of 0.1% Au/SnO_2-TiO_2 (4% Sn/Ti ratio) (Figure 4a). Under UV irradiation without catalyst, the decomposition of H_2O_2 has a linear relationship with time. In the presence of TiO_2, 0.1% Au/TiO_2 or 0.1% Au/SnO_2-TiO_2, the H_2O_2 decomposition was accelerated by

UV light, but the decomposition rate of H_2O_2 over 0.1% Au/SnO_2-TiO_2 is lower than TiO_2 and 0.1% Au/TiO_2. The relationship between hydrogen peroxide decomposition and time is nonlinear under UV irradiation, and the decomposition of H_2O_2 is similar to a one-order kinetics [30]. In order to investigate the decomposition solely induced by peroxide complexes, we tested the decomposition of H_2O_2 in an aqueous photocatalyst suspension with similar initial H_2O_2 concentrations under visible light irradiation (Figure 4b). H_2O_2 barely decomposed under dark conditions in an aqueous SnO_2-TiO_2 suspension or under visible light irradiation without any photocatalysts. In the presence of photocatalysts, the H_2O_2 decomposition was accelerated, but again, SnO_2 passivated TiO_2 had the lowest decomposition activity. All the decomposition processes under visible light irradiation can be roughly fitted with a near zero-order equation (linear relationship) [18]. It can be inferred that there is a synergistic effect between the photocatalysts and light irradiation in catalyzing H_2O_2 decomposition. However, SnO_2 passivated TiO_2 consistently showed suppressed decomposition activity in any condition (UV and visible light). It is important for SnO_2-TiO_2 heterojunction photocatalyst to maintain high and stable H_2O_2 production rate during the photocatalytic reaction. The generation and decomposition mechanism of H_2O_2 is shown in Figure 5. The electrons excited by UV light are transferred to the Au and SnO_2 to promote reduction of O_2 for H_2O_2 formation. Compared with easy H_2O_2 decomposition on pure TiO_2 via forming peroxide complexes, SnO_2 passivated TiO_2 suppressed H_2O_2 decomposition. Hence, this study provides a useful method for promoting H_2O_2 production over TiO_2 photocatalysts.

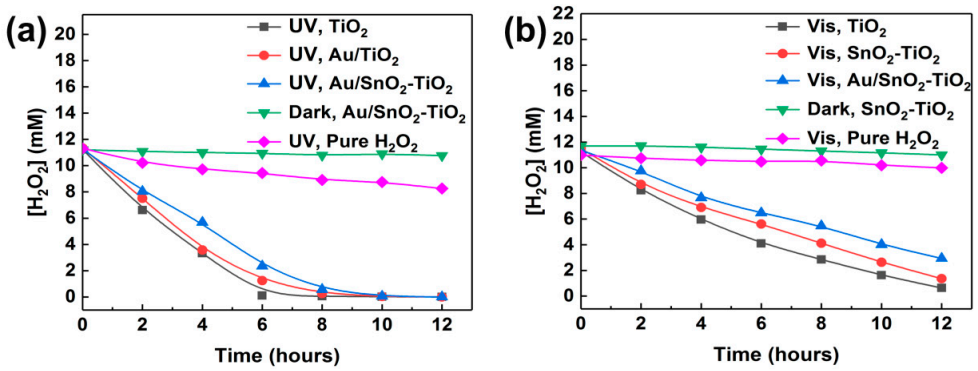

Figure 4. H_2O_2 photodecomposition under UV light (**a**) and visible light (**b**) conditions.

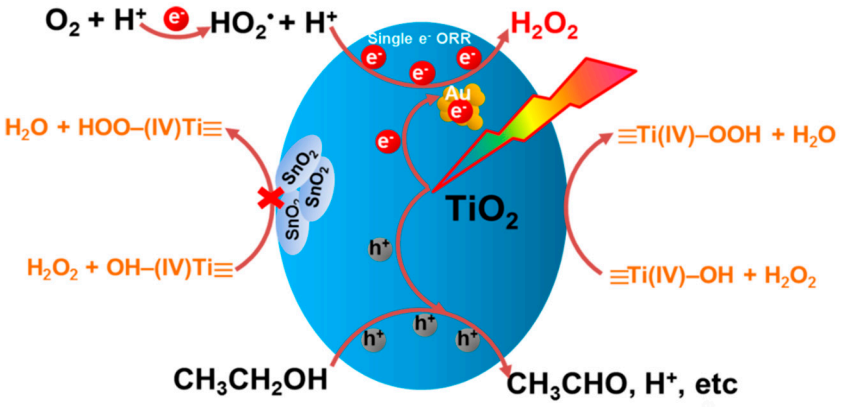

Figure 5. Schematic illustration of H_2O_2 synthesis and decomposition over Au/SnO_2-TiO_2.

3. Materials and Methods

3.1. Materials Preparation

To produce a SnO_2-TiO_2 heterojunction structure, anatase TiO_2 powder (with a grain size of 5 nm and a specific surface area of 280 m^2/g, Yifu Industrial Co., Ltd, Shanghai, China) was used as a photocatalyst. $SnCl_4 \bullet 4H_2O$ (Sinopharm Chemical Reagent Co., Ltd, Shanghai, China) was used to modify TiO_2 by a molten salt method. In general, 3.4 g anatase TiO_2 and 0.6 g $SnCl_4 \bullet 4H_2O$ (4% molar ratio of Sn:Ti) were mixed with 3.77 g LiCl (Yongda Chemical Reagent Co., Ltd, Tianjin, China) and 4.23 g KCl (Yongda Chemical Reagent Co., Ltd, Tianjin, China) in an alumina crucible. The powder mixtures were calcined at 500 °C, then the mixtures were transferred into the deionized water for grinding, centrifuged, washed and dried. The Au with 0.1 wt % was loaded on photocatalysts by the deposition-precipitation method reported previously [31]. The decomposition of H_2O_2 can be suppressed to a certain extent by sodium fluoride. SnO_2-TiO_2 can produce valence band electrons and holes by UV irradiation.

3.2. Material Characterization

The powder X-ray diffraction (XRD) data were collected on an X-ray diffractometer (D/Ma-2500, Rigaku, Tokyo, Japan) operating with Cu Kα radiation (λ = 0.15406 nm). UV-VIS spectra were recorded with a Spectrum Lambda 750 S (Perkin-Elmer, Waltham, MA, USA). High-resolution transmission electron microscopy (TEM) characterization was performed with 8000EX microscope (JEOL, Tokyo, Japan) operating at 200 kV.

3.3. Photocatalytic Reactivity Test

A photocatalytic reaction kettle (200 mL) was used as a photocatalytic reaction device. NaF (0.1 M, Shentai Chemical Reagent Co., Ltd, Tianjin, China) was added as part of reaction medium together with 0.2 g Au/SnO_2-TiO_2 into the reaction solution of alcohol (4 wt %) and deionized water. The suspension solution was under ultrasonic treatment for 2 to 3 min. Then the mixed solution was poured into the reaction kettle and the oxygen was passed for 30 min. Then, a 300 W Xe arc lamp (PLS-SXE300, Bofeilai Technology Co., Ltd, Beijing, China) was used as a light source and was turned on the solution. The light was emitted by the xenon lamp and reflected by the UV light reflector. Magnetic stirring of the suspension was maintained throughout the reaction. The condensate water continued to pass the reaction kettle. Then, the concentrations of H_2O_2 generated were determined by using the DMP (2,9-dimethyl-1,10-phenanthroline, Wengjiang Chemical Reagent Co., Ltd, Guangdong, China) method [27].

3.4. Quantification of H_2O_2 (DMP Method)

One mL of DMP (0.1 g/L), 1 mL of cupper (II) sulfate (0.1 M), and 1 mL of phosphate buffer (pH 7.0) solution, and 1 mL of reaction solution were added to a 10 mL volumetric flask and was mixed, and then deionized water was added to the volumetric flask to the tick mark. After mixing, the absorbance of the sample at 454 nm was measured. The blank solution was prepared in the same manner but without H_2O_2.

The concentrations of H_2O_2 were calculated by the following formula:

$$A_{454} = \zeta [H_2O_2] \times 1/10$$

where A_{454} is the difference of the absorbance between sample and blank solutions at 454 nm, ζ is the slope of the calibration curve, and $[H_2O_2]$ is the H_2O_2 concentration (μM).

3.5. Photocatalytic H_2O_2 Decomposition

Basically, photocatalytic H_2O_2 decomposition was carried out in the same reaction medium for photocatalytic H_2O_2 synthesis. Photocatalyst (0.2 g) was dispersed in water (200 mL) containing NaF (0.1 M), 4% C_2H_5OH (99.7%, Yongda Chemical Reagent Co., Ltd, Tianjin, China) and H_2O_2 (30%, Yongda Chemical Reagent Co., Ltd, Tianjin, China) with a fixed concentration. The suspension was stirred in the dark conditions for 30 min under constant N_2 bubbling to remove the air before light irradiation.

3.6. In Situ ESR Test

In situ electron spin resonance (ESR) analysis was performed to confirm the reduction pathway of O_2 over different catalysts, which uses 5,5-dimethyl-1-pyrroline N-oxide (DMPO) as a spin-trapping reagent. ESR signals of radicals trapped by DMPO were detected with a ESP 300E spectrometer (Brucker, Switzerland). Typically, catalyst (1 mg) was added to a mixture containing 1 mL alcohol/water (4 wt %) and 0.125 mmol DMPO. After passing the O_2 for 3 min, the sample was irradiated under UV light for 5 min before testing.

4. Conclusions

Au-modified SnO_2-TiO_2 was successfully prepared for enhanced photocatalytic activity for H_2O_2 production. The SnO_2-TiO_2 (4% SnO_2 modified anatase TiO_2) heterojunction prepared at 500 °C showed the best performance. H_2O_2 formed through a stepwise single electron reduction process over Au and/or SnO_2 modified TiO_2 via the formation of HO_2• intermediate. Under the band-gap excitation with UV light, decomposition of H_2O_2 seems to conform to a one-order kinetics process. SnO_2 passivation suppressed the decomposition of H_2O_2 over TiO_2 under both UV and visible light. This study provides a useful strategy to improve the performance of TiO_2 by modifying H_2O_2-inert oxide to decrease the decomposition of H_2O_2 during its photocatalytic synthesis.

Supplementary Materials: The following are available online at http://www.mdpi.com/2073-4344/9/7/623/s1, Figure S1: (TEM images of Au/SnO_2 TiO_2 and (b) EDX result of the square area in (a), Figure S2: (a) TEM images of Au/SnO_2 TiO_2 and (b) the measured interplanar spacing (0.235 nm) of Au (1 1 1) plane, Figure S3: Standard curve: a linear relationship for the optical absorbance at 454 nm as a function of H_2O_2 concentration, Figure S4: Plots of [H_2O_2] under UV-irradiation in the presence of different photocatalysts.

Author Contributions: G.Z., B.L. and Z.G. carried out the experimental work and prepared the manuscript. L.W., Y.D., and S.Z. tested the STEM of samples and provided useful suggestions to this work. The corresponding author X.M. directed the experimental work and paper writing. T.W. and V.A.L.R. were involved in the discussion and provided useful suggestions to this work. W.H. and F.Y. provided assistance in the test of in situ ESR and ICP-MS at Tianjin University. P.Z. and S.L. from the North China University of Science and Technology provided assistance with the experimental work.

Funding: This work was supported by the National Natural Science Foundation of China (51872091, 51502075, 21703065, and 51602153), "Hundred Talents Program" of Hebei Province (E2018050013), Natural Science Foundation of Hebei Province (B2018209267), Outstanding Youth Funds of North China University of Science and Technology (JP201604 and JQ201706), and the Hong Kong Scholars Program. Guifu Zuo, Bingdong Li, and Zhaoliang Guo contributed equally to this work.

Conflicts of Interest: There are no conflict to declare.

References

1. Sato, K.; Aoki, M.; Noyori, R. A "Green" Route to Adipic Acid: Direct Oxidation of Cyclohexenes with 30 Percent Hydrogen Peroxide. *Science* **1998**, *281*, 1646–1647. [CrossRef] [PubMed]
2. Samanta, C. Direct synthesis of hydrogen peroxide from hydrogen and oxygen: An overview of recent developments in the process. *Appl. Catal. A Gen.* **2008**, *350*, 133–149. [CrossRef]
3. Moon, G.H.; Kim, W.; Bokare, A.D.; Sung, N.E.; Choi, W. Solar production of H_2O_2 on reduced graphene oxide-TiO_2 hybrid photocatalysts consisting of earth-abundant elements only. *Energy Environ. Sci.* **2014**, *7*, 4023–4028. [CrossRef]

4. Domènech, X.; Ayllón, J.A.; Peral, J. H_2O_2 Formation from photocatalytic processes at the ZnO/water interface. *Environ. Sci. Pollut. Res.* **2001**, *8*, 285–287. [CrossRef]
5. Kormann, C.; Bahnemann, D.W.; Hoffmann, M.R. Environmental photochemistry: Is iron oxide (hematite) an active photocatalyst? A comparative study: α-Fe_2O_3, ZnO, TiO_2. *J. Photochem. Photobiol. A Chem.* **1989**, *48*, 161–169. [CrossRef]
6. Shi, L.; Yang, L.; Zhou, W.; Liu, Y.; Yin, L.; Hai, X.; Song, H.; Ye, J. Photoassisted Construction of Holey Defective g-C_3N_4 Photocatalysts for Efficient Visible-Light-Driven H_2O_2 Production. *Small* **2018**, *14*, 1703142. [CrossRef] [PubMed]
7. Shiraishi, Y.; Kanazawa, S.; Sugano, Y.; Tsukamoto, D.; Sakamoto, H.; Ichikawa, S.; Hirai, T. Highly Selective Production of Hydrogen Peroxide on Graphitic Carbon Nitride (g-C_3N_4) Photocatalyst Activated by Visible Light. *ACS Catal* **2016**, *4*, 774–780. [CrossRef]
8. Zhu, Z.; Pan, H.; Murugananthan, M.; Gong, J.; Zhang, Y. Visible light-driven photocatalytically active g-C_3N_4 material for enhanced generation of H_2O_2. *Appl. Catal. B Environ.* **2018**, *232*, 19–25. [CrossRef]
9. Zuo, G.; Liu, S.; Wang, L.; Song, H.; Zong, P.; Hou, W.; Li, B.; Guo, Z.; Meng, X.; Du, Y.; et al. Finely dispersed Au nanoparticles on graphitic carbon nitride as highly active photocatalyst for hydrogen peroxide production. *Catal. Commun.* **2019**, *123*, 69–72. [CrossRef]
10. Hirakawa, H.; Shiota, S.; Shiraishi, Y.; Sakamoto, H.; Hirai, T. Au Nanoparticles Supported on $BiVO_4$: Effective Inorganic Photocatalysts for H_2O_2 Production from Water and O_2 under Visible Light. *ACS Catal* **2016**, *6*, 4976–4982. [CrossRef]
11. Cai, R.; Kubota, Y.; Fujishima, A. Effect of copper ions on the formation of hydrogen peroxide from photocatalytic titanium dioxide particles. *J. Catal.* **2003**, *219*, 214–218. [CrossRef]
12. Daimon, T.; Hirakawa, T.; Kitazawa, M.; Suetake, J.; Nosaka, Y. Formation of singlet molecular oxygen associated with the formation of superoxide radicals in aqueous suspensions of TiO_2 photocatalysts. *Appl. Catal. A Gen.* **2008**, *340*, 169–175. [CrossRef]
13. Goto, H.; Hanada, Y.; Ohno, T.; Matsumura, M. Quantitative analysis of superoxide ion and hydrogen peroxide produced from molecular oxygen on photoirradiated TiO_2 particles. *J. Catal.* **2004**, *225*, 223–229. [CrossRef]
14. Zheng, L.; Su, H.; Zhang, J.; Walekar, L.S.; Vafaei, M.H.; Zhou, B.; Long, M.; Hu, Y.H. Highly selective photocatalytic production of H_2O_2 on sulfur and nitrogen co-doped graphene quantum dots tuned TiO_2. *Appl. Catal. B* **2018**, 475–484. [CrossRef]
15. Teranishi, M.; Naya, S.I.; Tada, H. In situ liquid phase synthesis of hydrogen peroxide from molecular oxygen using gold nanoparticle-loaded titanium(IV) dioxide photocatalyst. *J. Am. Chem. Soc.* **2010**, *132*, 7850–7851. [CrossRef]
16. Teranishi, M.; Naya, S.I.; Tada, H. Temperature-And pH-Dependences of In Situ Liquid-Phase Hydrogen Peroxide Formation from Molecular Oxygen by Gold Nanoparticle-Loaded Titanium (IV) Oxide Photocatalyst. *J. Phys. Chem. C* **2016**, *120*, 1083–1088. [CrossRef]
17. Tsukamoto, D.; Shiro, A.; Shiraishi, Y.; Sugano, Y.; Ichikawa, S.; Tanaka, S.; Hirai, T. Photocatalytic H_2O_2 Production from Ethanol/O_2 System Using TiO_2 Loaded with Au-Ag Bimetallic Alloy Nanoparticles. *ACS Catal.* **2012**, *2*, 599–603. [CrossRef]
18. Li, X.; Chen, C.; Zhao, J. Mechanism of Photodecomposition of H_2O_2 on TiO_2 Surfaces under Visible Light Irradiation. *Langmuir* **2001**, *17*, 4118–4122. [CrossRef]
19. Harbour, J.R.; Tromp, J.; Hair, M.L. Photogeneration of hydrogen peroxide in aqueous TiO_2 dispersions. *Can. J. Chem.* **1985**, *63*, 204–208. [CrossRef]
20. Kormann, C.; Bahnemann, D.W.; Hoffmann, M.R. Photocatalytic production of hydrogen peroxides and organic peroxides in aqueous suspensions of titanium dioxide, zinc oxide, and desert sand. *Environ. Sci. Technol.* **1988**, *22*, 798–806. [CrossRef]
21. Mendonça, V.R.D.; Avansi, W., Jr.; Arenal, R.; Ribeiro, C. A building blocks strategy for preparing photocatalytically active anatase TiO_2 /rutile SnO_2 heterostructures by hydrothermal annealing. *J. Colloid. Interface Sci.* **2018**, *505*, 454–459. [CrossRef]
22. Ohsaki, H.; Kanai, N.; Fukunaga, Y.; Suzuki, M.; Watanabe, T.; Hashimoto, K. Photocatalytic properties of SnO_2/TiO_2 multilayers. *Thin Solid Film.* **2006**, *502*, 138–142. [CrossRef]

23. Yuan, J.; Zhang, X.; Li, H.; Kai, W.; Gao, S.; Zhen, Y.; Yu, H.; Zhu, X.; Xiong, Z.; Xie, Y. TiO_2 /SnO_2 double-shelled hollow spheres-highly efficient photocatalyst for the degradation of rhodamine B. *Catal. Commun.* **2015**, *60*, 129–133. [CrossRef]
24. Naidu, H.P.; Virkar, A.V. Low-Temperature TiO_2-SnO_2 Phase Diagram Using the Molten-Salt Method. *J. Am. Ceram. Soc.* **2010**, *81*, 2176–2180. [CrossRef]
25. Jung, H.S.; Kim, H. Origin of low photocatalytic activity of rutile TiO_2. *Electron. Mater. Lett.* **2009**, *5*, 73–76. [CrossRef]
26. Alshammari, A.; Bagabas, A.; Assulami, M. Photodegradation of rhodamine B over semiconductor supported gold nanoparticles: The effect of semiconductor support identity. *Arab. J. Chem.* **2015**, *29*, 1–20. [CrossRef]
27. Kosaka, K.; Yamada, H.; Matsui, S.; Echigo, S.; Shishida, K. Comparison among the Methods for Hydrogen Peroxide Measurements To Evaluate Advanced Oxidation Processes: Application of a Spectrophotometric Method Using Copper(II) Ion and 2, 9-Dimethyl-1, 10-phenanthroline. *Environ. Sci. Technol.* **1998**, *32*, 3821–3824. [CrossRef]
28. Samira, S.; Arnau, V.C.; Mohammadreza, K.; Davide, D.; Paolo, M.; Björn, W.; María, E.E.; Paoli, E.A.; Rasmus, F.; Hansen, T.W. Enabling direct H_2O_2 production through rational electrocatalyst design. *Nat. Mater.* **2013**, *12*, 1137–1143.
29. Viswanathan, V.; Hansen, H.A.; Rossmeisl, J.; Nã¸Rskov, J.K. Unifying the 2e(-) and 4e(-) Reduction of Oxygen on Metal Surfaces. *J. Phys. Chem. Lett.* **2012**, *3*, 2948–2951. [CrossRef]
30. Maurino, V.; Minero, C.; Mariella, G.; Pelizzetti, E. Sustained production of H_2O_2 on irradiated TiO_2-fluoride systems. *Chem. Commun.* **2005**, *36*, 2627–2629. [CrossRef]
31. Liu, L.; Li, P.; Adisak, B.; Ouyang, S.; Umezawa, N.; Ye, J.; Kodiyath, R.; Tanabe, T.; Ramesh, G.V.; Ueda, S. Gold photosensitized $SrTiO_3$ for visible-light water oxidation induced by Au interband transitions. *J. Mater. Chem. A* **2014**, *2*, 9875–9882. [CrossRef]

© 2019 by the authors. Licensee MDPI, Basel, Switzerland. This article is an open access article distributed under the terms and conditions of the Creative Commons Attribution (CC BY) license (http://creativecommons.org/licenses/by/4.0/).